

# LETTERS TO THE EDITOR

The Letters to the Editor section is divided into four categories entitled Communications, Notes, Comments, and Errata. Communications are limited to three and one half journal pages, and Notes, Comments, and Errata are limited to one and three-fourths journal pages as described in the Announcement in the 1 July 1995 issue.

## COMMUNICATIONS

### Electronic control of the spin-orbit branching ratio in the photodissociation and predissociation of HCl

Rohana Liyanage, Yung-an Yang,<sup>a)</sup> Satoshi Hashimoto,<sup>b)</sup> and Robert J. Gordon  
Department of Chemistry, University of Illinois at Chicago, Chicago, Illinois 60607-7061

Robert W. Field

Department of Chemistry, Massachusetts Institute of Technology, Cambridge, Massachusetts 02139

(Received 6 July 1995; accepted 11 August 1995)

The fine structure branching ratio of chlorine atoms produced in the photodissociation and predissociation of HCl was measured for excitation energies between 51 800 and 83 800 cm<sup>-1</sup>. The branching ratio between 60 000 and 70 000 cm<sup>-1</sup> is in good agreement with the calculations of Alexander *et al.* [J. Chem. Phys. **99**, 1752 (1993)], converging to the statistical limit at high energy. Predissociation of electronically excited bound states display a surprisingly rich behavior, demonstrating that the nature of the predissociating continuum state has a large effect on the atom fragment branching ratio. © 1995 American Institute of Physics.

The relative populations of the fine-structure states of fragment atoms provide valuable information for understanding the nonadiabatic processes involved in the dissociation of electronically excited molecules. The two main factors which determine the product branching ratio are the structure of the excited state wave function in the Franck-Condon region where dissociation is initiated, and the couplings between potential energy surfaces at large distances where the separation between molecular states is comparable to the fragment spin-orbit splitting. A key dynamical parameter is the ratio of the recoil time to the spin-orbit precession period,

$$\xi = \frac{R\Delta E_{SO}}{v\hbar}, \quad (1)$$

where  $R$  is the width of the recoupling region,  $\Delta E_{SO}$  is the spin-orbit splitting, and  $v$  is the recoil velocity.<sup>1</sup> If this adiabaticity parameter is large, we expect the fragment atomic spin-orbit states to correlate adiabatically with the molecular states populated by the excitation pulse, while if it is small a statistical (or more correctly, a diabatic) distribution is anticipated.

Because of the relative simplicity of its electronic structure, HCl is an ideal case for comparing theory and experiment. Potential energy curves for all the low-lying excited states of HCl are shown in Fig. 1.<sup>2</sup> The leading orbital configurations of the  $X^1\Sigma^+$  ground state are  $4\sigma^25\sigma^22\pi^4$  at short distances, corresponding to the ionic  $H^+Cl^-$  structure, and the covalent  $4\sigma^25\sigma^16\sigma^12\pi^4$  configuration at long distances. Promotion of a  $2\pi$  electron in the ionic configuration to the  $6\sigma$  antibonding orbital generates the  $a^3\Pi_i$  and  $A^1\Pi$  con-

tinuum valence states, producing a broad, structureless absorption between 50 000 and 70 000 cm<sup>-1</sup>. Promotion instead of a  $5\sigma$  electron to the  $6\sigma$  orbital produces the  $t^3\Sigma^+$  continuum state and the  $V^1\Sigma^+$  bound state.<sup>3,4</sup> All the other curves in Fig. 1 correspond to bound Rydberg states with nominal  $(X^2\Pi_i)n/l\lambda$  configurations.<sup>5</sup>

All previous work on the spin-orbit branching ratio for HCl dealt with the  $A^1\Pi$  continuum state. It is readily shown that the  $X^1\Sigma^+$ ,  $A^1\Pi$ ,  $a^3\Pi_2$ ,  $a^3\Pi_1$ , and  $a^3\Pi_0-$  states correlate adiabatically with  $H(^2S)+Cl(^2P_{3/2})$ , while the  $t^3\Sigma^+$  and  $a^3\Pi_{0+}$  states correlate with  $H(^2S)+Cl(^2P_{1/2})$ .<sup>6</sup> (See Table I.) Since most of the oscillator strength is carried by the  $A^1\Pi \leftarrow X^1\Sigma^+$  transition, the adiabatic fragments are primarily  $H(^2S)+Cl(^2P_{3/2})$ . Nonadiabatic transitions to produce  $Cl(^2P_{1/2})$  may nevertheless occur, since  $\xi$  is small and all of the continuum states are coupled by the rotation and spin-orbit terms in the Hamiltonian.<sup>7</sup> In the diabatic limit (Table I), all of the states except for  $a^3\Pi_2$  correlate with both spin-orbit states.

A calculation performed by Givertz and Balint-Kurti (GB)<sup>8</sup> ignoring rotational coupling predicted a smooth increase of the branching ratio

$$\Gamma = \frac{[Cl(^2P_{1/2})]}{[Cl(^2P_{1/2})] + [Cl(^2P_{3/2})]} \quad (2)$$

from 0.21 at 53 500 cm<sup>-1</sup> to 0.31 at 75 200 cm<sup>-1</sup>. These values may be compared with the statistical limit of  $\Gamma=1/3$ , which is defined as the ratio of the degeneracy of  $Cl(^2P_{1/2})$  to the sum of the degeneracies of both fine structure states.

Recently Alexander *et al.* (APD)<sup>9</sup> reported a calculation using more accurate potential energy functions and including rotational coupling between all of the states. Although they found that rotational coupling has a negligible effect on  $\Gamma$ , their branching ratios were nevertheless considerably larger

<sup>a)</sup>Permanent address: DOTY Scientific, Inc, 700 Clemson Rd., Columbia, SC 29223.

<sup>b)</sup>Permanent address: Institute for Electronic Science, Hokkaido University, Sapporo 060, Japan.

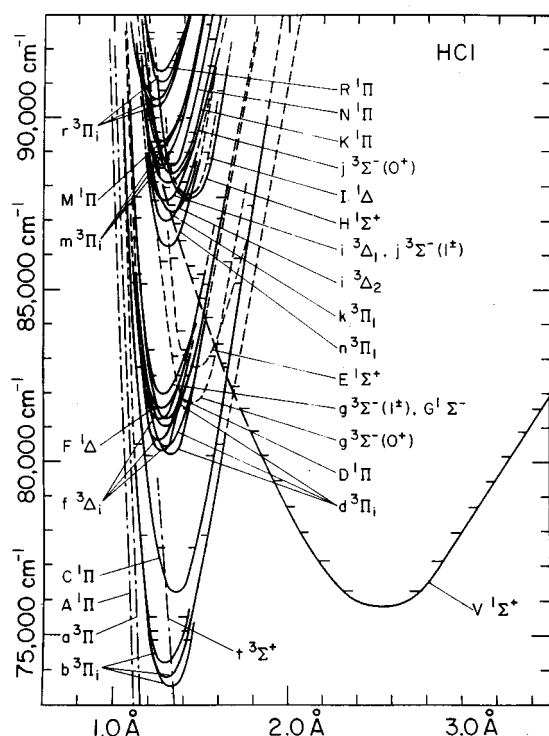


FIG. 1. Diabatic potential energy curves for HCl.

than those of GB. Moreover, they found that  $\Gamma$  decreases over the experimental range of energies, approaching the statistical limit from above.

Experimental measurements at  $51\,800\text{ cm}^{-1}$  (193 nm) reported by several groups<sup>6,10,11</sup> gave a statistical product ratio, which lies between the predictions of the two calculations, while measurements by Tonokura *et al.*<sup>6</sup> at  $63\,700\text{ cm}^{-1}$  (157 nm) gave a value of  $\Gamma=0.47\pm 0.04$ , which is larger than the predictions of both calculations. In view of the discrepancies among the previous studies, and particularly because of the experimental evidence that at high energy  $\Gamma$  exceeds the statistical limit, it is desirable to extend the energy range of the measurements. In particular, we would like to know if, as naively expected,  $\Gamma$  eventually reaches the diabatic limit at higher energy.

Previous measurements of  $\Gamma$  were limited to wavelengths of 193 and 157 nm, which are readily generated with excimer lasers. In order to extend the energy range of  $\Gamma$ , we performed two types of experiments. First, we studied the

TABLE I. Adiabatic and diabatic correlation of the continuum states of HCl.

State <sup>a</sup>	Adiabatic limit		Diabatic limit	
	Cl( <sup>2</sup> P <sub>1/2</sub> )	Cl( <sup>2</sup> P <sub>3/2</sub> )	Cl( <sup>2</sup> P <sub>1/2</sub> )	Cl( <sup>2</sup> P <sub>3/2</sub> )
A <sup>1</sup> Π <sub>1</sub> (e,f)	0	1	1/3	2/3
a <sup>3</sup> Π <sub>0</sub> <sup>+</sup> (e)	1	0	2/3	1/3
a <sup>3</sup> Π <sub>0</sub> <sup>-</sup> (f)	0	1	2/3	1/3
a <sup>3</sup> Π <sub>1</sub> (e,f)	0	1	1/3	2/3
a <sup>3</sup> Π <sub>2</sub> (e,f)	0	1	0	1
t <sup>3</sup> Σ <sub>0</sub> <sup>+</sup> (f)	1	0	1/3	2/3
t <sup>3</sup> Σ <sub>1</sub> <sup>+</sup> (e,f)	1	0	1/3	2/3

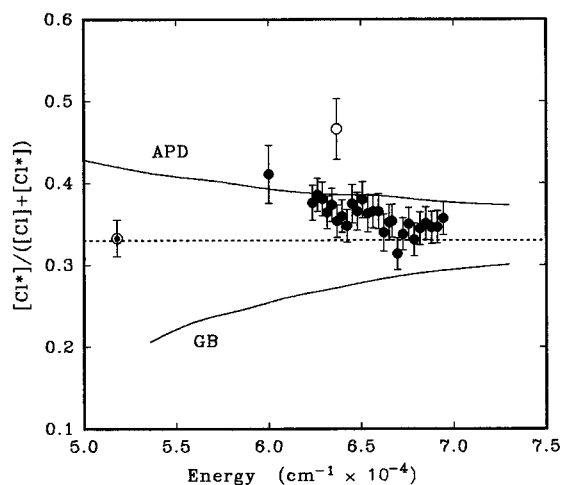
<sup>a</sup>e and f refer to the parity of the electronic states.

FIG. 2. Fine-structure branching ratio for the photodissociation of HCl as a function of excitation energy. Filled circles above  $60\,000\text{ cm}^{-1}$  were obtained by three-photon excitation. The data point  $51\,800\text{ cm}^{-1}$  is the calibration measurement of Refs. 6, 10, and 11. The open circle is the measurement of Tonokura *et al.* in Ref. 6. The error bars are single standard deviations. The solid curves labeled APD and GB are the calculations of Alexander *et al.* (Ref. 9) and Givertz and Balint-Kurti (Ref. 8), respectively. The dotted line is the statistical limit.

direct photodissociation of HCl between  $60\,000$  and  $69\,500\text{ cm}^{-1}$ , using three photons to excite the A <sup>1</sup>Π state. Second, we studied the predissociation of HCl between  $77\,500$  and  $83\,800\text{ cm}^{-1}$ , using two photons to excite discrete rotational levels of various Rydberg states and the V <sup>1</sup>Σ<sup>+</sup> ( $v'=10$ ) valence state. The second set of measurements allowed us also to study the effect of rotational angular momentum on the Cl fine-structure branching ratio.

These experiments were performed using a pump-and-probe apparatus, which has been described previously.<sup>12</sup> Briefly, a tunable excimer-pumped dye laser was used to excite HCl, while a second tunable dye laser was used to probe the neutral Cl fragment by means of resonance-enhanced multiple photon ionization (REMPI), using the  $4p\ ^2D_{3/2} \leftarrow 3p\ ^2P_{3/2}$  transition for Cl(<sup>2</sup>P<sub>3/2</sub>) and  $4p\ ^2P_{1/2} \leftarrow 3p\ ^2P_{1/2}$  for Cl(<sup>2</sup>P<sub>1/2</sub>).<sup>13</sup> Details specific to this experiment will be provided in a future publication.

The results of the first experiment are shown in Fig. 2. These data display the high-energy behavior predicted by APD, converging from above to the statistical limit. For  $R\approx 1.5$  bohr (see Fig. 6 of Ref. 9),  $\xi$  lies in the range of 0.5–0.7, which is consistent with diabatic behavior. The discrepancy between theory and experiment at  $51\,800\text{ cm}^{-1}$  remains unexplained.

All of the measurements in Fig. 2 were scaled to the measured value of  $\Gamma=1/3$  at  $51\,800\text{ cm}^{-1}$ .<sup>14</sup> This calibration is especially reliable since two of the previous measurements<sup>10,11</sup> at this energy were sensitive to deviations from a nonstatistical atomic fine-structure ratio, and none was detected. Another point to be considered is our use of three photons to excite HCl. The rotational selection rule for a  $\Pi \leftarrow \Sigma$  transition is  $\Delta J=0, \pm 1$  for one photon and  $0, \pm 1, \pm 2, \pm 3$ , for three photons. The larger range of  $J$  accessible with three photons is unlikely to have a measurable effect on  $\Gamma$  because the rotational line strengths for  $|\Delta J|=2$  and 3 are

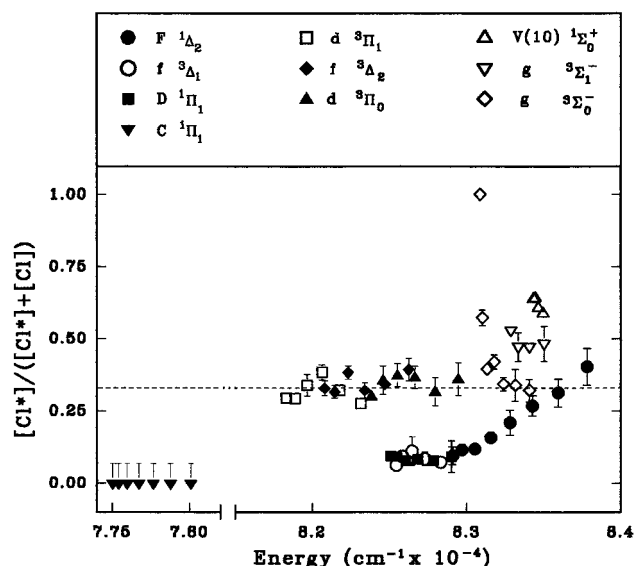


FIG. 3. Fine-structure branching ratio for the predissociation of HCl as a function of excitation energy. The three classes of states are listed in the columns above the figure. All of the electronic states are vibrationless, except for  $V\ ^1\Sigma^+(v'=10)$ . The dotted line is the statistical limit.

an order of magnitude smaller than those for  $|\Delta J|=1$ .<sup>15</sup> Moreover, APD showed that rotational coupling should have a negligible effect on  $\Gamma$ , and any such effect would be even further diminished by thermal averaging at 300 K.

Another possible consequence of using three photons is excitation to the  $a\ ^3\Pi$  state. For a single-photon transition, APD showed that the  $a\ ^3\Pi$  state carries  $<0.5\%$  of the oscillator strength. While it is conceivable that the rate of the spin-forbidden transition to this state may be greater for three photons, it is unlikely that this is a large effect since there are no nearby states that could lend oscillator strength in a perturbation expansion of the transition matrix element.<sup>16</sup>

The branching ratios for predissociation at high energy are shown in Fig. 3. From the data in Fig. 2 we anticipated that  $\Gamma$  would be diabatic at still higher energy (where  $\xi \leq 0.4$ ). The only continuum state that intersects the bound states that we studied is  $t\ ^3\Sigma^+$ . Although this state correlates with  $\text{Cl}(^2P_{1/2})$ , the shorter recoil time at high energy is expected to produce a statistical population. In light of this reasoning, the data shown in Fig. 3 are very surprising. Depending on the choice of the initially excited gateway (i.e., predissociating) state, nearly every type of behavior imaginable was observed.

The branching ratios plotted in Fig. 3 fall into three phenomenological cases: (i) The  $d\ ^3\Pi_0$ ,  $d\ ^3\Pi_1$ , and  $f\ ^3\Delta_2$  states exhibit statistical branching ratios, which appear to be a continuation of the  $A\ ^1\Pi$  data shown in Fig. 2. (ii) The  $C\ ^1\Pi_1$ ,  $D\ ^1\Pi_1$ ,  $f\ ^3\Delta_1$ , and  $F\ ^1\Delta_2$  (at low  $J$ ) states have  $\Gamma$  close to zero. For the  $C$  state no  $\text{Cl}(^2P_{1/2})$  was detectable, with an upper bound on  $\Gamma$  of 10%. The  $F$  state is anomalous in that it displays a marked  $J$ -dependence, with  $\Gamma$  increasing smoothly from 0.1 at  $J'=2$  to 0.4 at  $J'=9$ . (iii) The  $g\ ^3\Sigma_1^-$ ,  $g\ ^3\Sigma_0^-$ , and  $V\ ^1\Sigma^+(v'=10)$  states display Cl fine-structure population inversions. For the  $g\ ^3\Sigma_0^-$  state there is a strong inverse  $J$ -dependence, with  $\Gamma=1$  for  $J'=0$ . In addition,

there were several states from which no Cl was detected in either fine-structure state. For the  $E\ ^1\Sigma_0^+$  state a strong  $\text{HCl}^+$  parent ion signal was observed. Since this state is strongly spin-orbit coupled to other  $\Omega=0^+$  states, it is surprising that no Cl was observed. In the case of the  $f\ ^3\Delta_3$  state, the  $\text{HCl}^+$  signal was very weak, and the absence of Cl may be due simply to weak absorption by the molecule. The same may also be true for the  $d\ ^3\Pi_2$  state, for which we saw no  $\text{HCl}^+$  parent ion signal.

Before attempting to explain the energy dependence of  $\Gamma$ , it is necessary to establish the mechanism for Cl production. In the case of  $F\ ^1\Delta$  we have shown that Cl is produced by indirect predissociation,<sup>17</sup> resulting from a coupling of  $F\ ^1\Delta$  to both  $C\ ^1\Pi(v=2)$  and  $b\ ^3\Pi_i(v=3)$ , with the latter serving as gateway states to the  $t\ ^3\Sigma^+$  and/or the  $A\ ^1\Pi$  continua. The other states listed in Fig. 3 are also perturbed by these continua. The important point is that in each case predissociation occurs after absorption of two photons, at the energies shown in Fig. 3. A series of experiments was performed to rule out possible three- and four-photon mechanisms. Those experiments, which include measurement of the Cl recoil speed by velocity-aligned Doppler spectroscopy and intensity measurements of parent and fragment REMPI peaks, will be reported in detail in a future publication. In every case, two-photon excitation was found to be the dominant mechanism.

It is generally agreed that for small  $\xi$  the fragment spin-orbit branching ratio depends on the coupling of closely lying potential energy curves at large distances. This mechanism is clearly demonstrated in the flux calculations of APD.<sup>18</sup> What has not been established is the influence of the Franck-Condon region on the final-state distribution. An overly simple view of photodissociation would suggest that the dynamics at short distances (i.e., in the Franck-Condon region) has less of an effect on  $\Gamma$  than at large distances, apart from determining the asymptotic recoil energy. From such a naive perspective, predissociated Rydberg states should produce Cl atoms with the diabatic fine-structure populations characteristic of the predissociating continuum state.

That this picture is too simple is already evident in the calculations of APD, who found different high-energy behavior for HCl vs DCl excited to the same continuum state.<sup>18</sup> Our present results demonstrate the failure of this model even more dramatically, where different gateway states produce radically different dependencies of  $\Gamma$  on energy and rotational angular momentum.

We cannot presently rationalize many of the details of Fig. 3. Why, for example, does  $f\ ^3\Delta_1$  belong to case (ii) while  $f\ ^3\Delta_2$  belongs to case (i)? Also we do not know the cause of the  $J$ -dependence of the  $F\ ^1\Delta$  state. On a less detailed level, however, some patterns may be recognized, using the *adiabatic* picture. The unique behavior of the  $g\ ^3\Sigma_0^-$  state, for which  $\Gamma$  varies inversely with  $J$ , can be explained by its parity. Since this state has (*e*) parity, the only continuum state with which it interacts at  $J=0$  is  $a\ ^3\Pi_0^+$ , which correlates adiabatically with  $\text{Cl}(^2P_{1/2})$ .<sup>19</sup> For  $J>0$ ,  $S$ -uncoupling mixes the  $g\ ^3\Sigma_0^-$  and  $g\ ^3\Sigma_1^-$  states, and, since the latter couples with  $a\ ^3\Pi_1$ , both fine-structure states of Cl may be

produced. The high  $\text{Cl}(^2P_{1/2})$  population for the other two states in group (iii) is understandable because they are both mixed with  $g\ ^3\Sigma_0^-$  for  $J > 0$ .

The large population of  $\text{Cl}(^2P_{3/2})$  for cases (i) and (ii) may be explained by the adiabatic correlation of the  $A\ ^1\Pi$  and  $a\ ^3\Pi_{0-1,2}$  continua. We know, for example, that  $F\ ^1\Delta$  is predissociated by  $C\ ^1\Pi_1$  and  $b\ ^3\Pi_1$  via  $L$ -uncoupling and  $l$ -mixing.<sup>17</sup> We further expect that  $A\ ^1\Pi$  and  $a\ ^3\Pi_1$  are strongly coupled to  $C\ ^1\Pi$  and  $b\ ^3\Pi_1$  by electrostatic interaction.<sup>20,21</sup> Direct coupling of the  $C$  and  $b$  states to  $t\ ^3\Sigma^+$ , which correlates with  $\text{Cl}(^2P_{1/2})$ , is less likely than via the  $a$ ,  $A$  states, despite large Franck–Condon overlap factors, because the configurations of these states differ by two orbitals. We further expect that the  $D\ ^1\Pi$  and ( $C\ ^1\Pi, b\ ^3\Pi_1$ ) states are coupled by  $l$ -mixing,<sup>17</sup> and that the singlet and triplet pairs ( $A \sim a$ ,  $C \sim b$ ,  $D \sim d$ ) are coupled by the spin–orbit operator. Hence, the observation of more  $\text{Cl}(^2P_{3/2})$  for the  $D$  state is justified.

Predissociation of the Rydberg states of HCl is further complicated by interaction with the  $e\ ^3\Sigma^+$  state, which has an origin in the vicinity of  $81\ 000\ \text{cm}^{-1}$  (Ref. 22) and undergoes an avoided crossing with the  $t\ ^3\Sigma^+$  state.<sup>3,4,23</sup> The  $e$  state is the only Rydberg state below  $90\ 000\ \text{cm}^{-1}$  that has never been vibrationally resolved (and hence is not shown in Fig. 1), presumably because of its strong predissociation by the  $t$  state.<sup>24</sup> Spin–orbit interaction couples  $e\ ^3\Sigma_1^+$  to  $g\ ^3\Sigma_1^-$ ,  $d\ ^3\Pi_1$ , and  $D\ ^1\Pi_1$ , and  $e\ ^3\Sigma_0^+$  to  $d\ ^3\Pi_0$ . This interaction provides a pathway to the  $t\ ^3\Sigma^+$  state, which correlates adiabatically to  $\text{Cl}(^2P_{1/2})$ . From the electronic origins of these states,<sup>25</sup> we estimate that  $D\ ^1\Pi(v=0)$  is more likely to be perturbed electrostatically by  $C\ ^1\Pi(v=2)$ , while  $d\ ^3\Pi_{0,1}$  are spin–orbit perturbed by  $e\ ^3\Sigma_{0,1}^+$ . These perturbations may explain why the  $D$  and  $d$  states have different spin–orbit branching ratios (Fig. 3).

In conclusion, we have demonstrated that both adiabatic and diabatic mechanisms are important in determining the fine-structure population of photofragments. For direct photodissociation we found that the diabatic picture predicts the branching ratio. For predissociation of bound states, both perturbations in the Franck–Condon region and adiabatic correlation play a role. By selecting the initially excited “gateway” state, it is possible to control passively the outcome of a photoinduced dissociation reaction.

We wish to thank Professor H el ene Lefebvre-Brion for a number of helpful discussions. We also wish to thank Professor Marshall Ginter and Dr. Dorothy Ginter for providing us with Fig. 1. Support by the National Science Foundation under Grant Nos. CHE-9408801 and PHY-9206064 is gratefully acknowledged.

<sup>1</sup>Y.-L. Huang and R. J. Gordon, *J. Chem. Phys.* **94**, 2640 (1991), and references cited therein.

<sup>2</sup>This figure was kindly provided by M. L. Ginter and D. L. Ginter.

<sup>3</sup>E. F. Van Dishoeck, M. C. van Hemert, and A. Dalgarno, *J. Chem. Phys.* **77**, 3693 (1982).

<sup>4</sup>M. Bettendorff, S. D. Peyerimhoff, and R. J. Buenker, *Chem. Phys.* **66**, 261 (1982).

<sup>5</sup>D. S. Ginter and M. L. Ginter, *J. Mol. Spectrosc.* **90**, 177 (1992).

<sup>6</sup>K. Tonokura, Y. Matsumi, M. Kawasaki, S. Tasaki, and R. Bersohn, *J. Chem. Phys.* **97**, 8210 (1992).

<sup>7</sup>H. Lefebvre-Brion and R. W. Field, *Perturbations in the Spectra of Diatomic Molecules* (Academic, New York, 1986).

<sup>8</sup>S. C. Givertz and G. G. Balint-Kurti, *J. Chem. Soc. Faraday Trans. 2* **82**, 1231 (1986).

<sup>9</sup>M. H. Alexander, B. Pouilly, and T. Duhoo, *J. Chem. Phys.* **99**, 1752 (1993).

<sup>10</sup>E. Tiemann, H. Kanamori, and E. Hirota, *J. Chem. Phys.* **88**, 2457 (1988).

<sup>11</sup>J. Park, Y. Lee, and G. W. Flynn, *Chem. Phys. Lett.* **186**, 441 (1991).

<sup>12</sup>P. T. A. Reilly, Y. Xie, and R. J. Gordon, *Chem. Phys. Lett.* **178**, 511 (1991).

<sup>13</sup>S. Arepalli, N. Presser, D. Robie, and R. J. Gordon, *Chem. Phys. Lett.* **118**, 88 (1985).

<sup>14</sup>The ratio of ion signals that we measured at  $51\ 800\ \text{cm}^{-1}$  (193 nm) using the  $4p\ ^2D_{3/2} \rightarrow 3p\ ^2P_{3/2}$  and  $4p\ ^2D_{3/2} \leftarrow 3p\ ^2P_{1/2}$  transitions is in quantitative agreement with the ratio reported in Ref. 6. The signal intensity ratio measured for these transitions was multiplied by a factor of  $2.5 \pm 0.1$  in order to obtain  $\Gamma = 1/3$ , as prescribed in Table II of Ref. 6. For the  $4p\ ^2D_{3/2} \leftarrow 3p\ ^2P_{3/2}$  and  $4p\ ^2P_{1/2} \leftarrow 3p\ ^2P_{1/2}$  transitions used routinely at all photolysis wavelengths, the appropriate calibration factor is  $0.85 \pm 0.10$ .

<sup>15</sup>J. B. Halpern, H. Zacharias, and R. Wallenstein, *J. Mol. Spectrosc.* **79**, 1 (1980).

<sup>16</sup>A crude estimate of the  $a\ ^3\Pi_1$  triplet amplitude in the three-photon virtual state is given by the ratio of the  $A\ ^1\Pi \sim a\ ^3\Pi_1$  spin–orbit matrix element to the energy defect between  $nh\nu$  ( $n = 1$  or  $2$ ) and the energy of  $a\ ^3\Pi_1$  at  $r_e(X\ ^1\Sigma^+) = 1.27\ \text{Å}$ , namely 0.008 for  $n = 1$  and 0.020 for  $n = 2$ .

<sup>17</sup>R. Liyanage, P. T. A. Reilly, Y.-A. Yang, R. J. Gordon, and R. W. Field, *Chem. Phys. Lett.* **216**, 554 (1993).

<sup>18</sup>See Figs. 6 and 7 of Ref. 9.

<sup>19</sup>The  $g\ ^3\Sigma_0^-$  state can mix with both  $V\ ^1\Sigma^+$  and  $a\ ^3\Pi_{0+}$  at  $j = 0$ . The  $g \sim V$  spin–orbit perturbation cannot introduce a  $J$ -dependence of  $\Gamma$ , but the  $J$ -dependence of the  $g\ ^3\Sigma_0^- \sim g\ ^3\Sigma_1^-$  mixing together with the  $g\ ^3\Sigma_1^- \sim a\ ^3\Pi_1$  perturbation can produce such an effect.

<sup>20</sup>A. W. Yench, D. Kaur, R. J. Donovan, A. Kvaran, A. Hopink, H. Lefebvre-Brion, and F. Keller, *J. Chem. Phys.* **99**, 4986 (1993).

<sup>21</sup>The electrostatic coupling matrix element between the  $^1\Sigma^+(A\ ^2\Sigma^+, 4s\sigma)$  and the  $V\ ^1\Sigma^+(A\ ^2\Sigma^+, \sigma^*)$  states is  $7000\ \text{cm}^{-1}$  (see Ref. 20). We expect the  $C\ ^1\Pi(X^2\Pi, 4s\sigma)$  and the  $A\ ^1\Pi(X^2\Pi, \sigma^*)$  states to be comparably strongly coupled; H. Lefebvre-Brion (private communication).

<sup>22</sup>J. Jureta, S. Cvejanović, D. Cvejanović, M. Kurepa, and D. Čubric, *J. Phys. B*, **22**, 2623 (1989).

<sup>23</sup>In Refs. 3 and 4 the  $t$  and  $e$  states are labeled  $1\ ^3\Sigma^+$  and  $2\ ^3\Sigma^+$ , respectively.

<sup>24</sup>S. G. Tilford and M. L. Ginter, *J. Mol. Spectrosc.* **40**, 568 (1971).

<sup>25</sup>F. R. Greening, *Chem. Phys. Lett.* **34**, 581 (1975); D. S. Green and S. C. Wallace, *J. Chem. Phys.* **96**, 5857 (1992).